# ENERGY STORAGE EFFICIENCY FOR THE AMMONIA/HYDROGEN-NITROGEN THERMOCHEMICAL ENERGY TRANSFER SYSTEM

BY

O M WILLIAMS AND P O CARDEN

DEPARTMENT OF ENGINEERING PHYSICS

RESEARCH SCHOOL OF PHYSICAL SCIENCES

THE AUSTRALIAN NATIONAL UNIVERSITY

CANBERRA, A.C.T., AUSTRALIA

SUBMITTED TO THE INTERNATIONAL JOURNAL OF ENERGY RESEARCH

JULY 1978

# ENERGY STORAGE EFFICIENCY FOR THE AMMONIA/HYDROGEN-NITROGEN THERMOCHEMICAL ENERGY TRANSFER SYSTEM

by

O M Williams and P O Carden

Department of Engineering Physics
Research School of Physical Sciences
The Australian National University
Canberra, A.C.T., AUSTRALIA

ABSTRACT

Energy storage efficiency is calculated for the solar thermochemical energy transfer system based on ammonia/hydrogen-nitrogen. The calculation for this system involves generation of thermodynamic data not available in the literature by a method in which use is made of the available phase equilibrium measurements together with application of the criterion that the correct value of separation work for a two-phase mixture must be generated internally by degradation of mixing heat. Energy storage efficiencies for ammonia/hydrogen-nitrogen are derived from the generated thermodynamic data and are shown to increase towards unity as the endothermic

reaction approaches completion, with efficiencies greater than 0.90 being obtained for reaction extents exceeding 0.60. The validity of the analysis has been tested successfully by comparison between the thermodynamic predictions and experimental data in the form of measurements of the waste heat rejected from a counterflow heat exchanger operated with liquid ammonia feed and ammonia/hydrogen-nitrogen output.

# INTRODUCTION

In the preceding paper (Carden and Williams [1]) we have derived expressions which enable the thermodynamic efficiency of a liquid/gas separating thermochemical energy transfer system to be evaluated. The analysis has been oriented towards the anticipated operation of a thermochemical system within a large scale solar power plant based on a distributed array of concentrating collectors. The overall efficiency for such a system may be divided into two factors: a work recovery efficiency associated with the operation of the central exothermic reactor, and an energy storage efficiency related to the amount of energy rejected at the individual endothermic reactors in the form of low grade heat wasted to the environment.

Calculation of work recovery efficiencies for a given separating thermochemical system requires no more thermodynamic information than for the pure reaction components. In contrast, detailed thermodynamic data is required for both the components and their mixtures for the calculation of energy storage efficiencies, particularly in the region of the boundary separating single-phase and two-phase mixtures. This latter information is not readily available within the chemical engineering literature even for such industrially important systems as ammonia/hydrogen-nitrogen. Phase equilibrium data defining the compositions of the liquid and gas phases may be available but there is a paucity of data for determining mixture values for the thermodynamically important variables such as enthalpy and Gibbs' free energy.

In this paper we describe a method for generating the thermodynamic data necessary for calculation of energy storage efficiencies. The method is based on the combined use of phase equilibrium data and the requirement that the system be thermodynamically consistent in that the correct value of separation work for a given mixture be developed internally by degradation of mixing heat. Energy storage efficiencies are calculated for the ammonia dissociation/synthesis system proposed by Carden [2] and the variation with endothermic reaction extent is discussed from the point of view of optimising system operation towards maximum efficiency. It is found that energy storage efficiencies increase towards unity as the reaction extent increases and that efficiencies in excess of 0.90 are readily achievable for a practical thermochemical energy transfer system based on the ammonia dissociation/synthesis reaction. The validity of the analysis has been tested successfully by comparison between the thermodynamic predictions and experimental data in the form of measurements of the waste heat rejected from a counterflow heat exchanger operated with liquid ammonia feed and ammonia/ hydrogen-nitrogen output.

## 2. THERMODYNAMIC DATA FOR AMMONIA/HYDROGEN-NITROGEN

The energy storage efficiency $\eta_{ST}$ for the liquid/gas thermochemical reaction

$$A \rightleftharpoons mB \quad , \quad \Delta H^\circ > 0 \qquad (1)$$

is defined in [1] for a distributed solar power plant as

$$\eta_{ST} = \Delta H(T_S)/\Delta H_{max} \tag{2}$$

where $T_S$ is the temperature of the fluid fed to the counterflow heat exchanger associated with the endothermic reactor, and where $\Delta H(T_S)$ is the enthalpy difference between the feed and return fluids. The denominator in (2) represents the maximum value of $\Delta H(T)$ throughout the temperature range of the heat exchanger. Since the thermodynamic data available in the literature is incomplete for the ammonia/hydrogen-nitrogen reaction

$$NH_3 \rightleftharpoons \frac{3}{2}H_2 + \frac{1}{2}N_2 \tag{3}$$

the essential problem in the present study amounts to developing a procedure for generating enthalpies for mixtures of ammonia and 3:1 hydrogen-nitrogen so that the enthalpy differences in (2) and hence $\eta_{ST}$ may be evaluated. As in [1], each mixture is characterized by the mole fraction x of the gas mixture, or alternatively by the weight fraction $\delta$, where

$$\delta = \frac{x}{m(1 - x) + x} \tag{4}$$

with m = 2 for the reaction (3). In the following sections we survey the available thermodynamic literature for the ammonia/hydrogen-nitrogen system and, where it is incomplete, we calculate mixture enthalpies by a method based on the equality of separation work and the loop work developed by degradation of mixing heat.

## 2.1 Literature Survey

Thermodynamic data for ammonia, hydrogen and nitrogen appear in various standard reference texts [3, 4] but often do not cover the entire temperature range of interest in the present study, particularly within the high pressure region. The required data have been collated elsewhere (Williams [5]) and supplemented by corresponding states principle correlations. Ammonia above 500 K is well represented on a corresponding states basis if effective critical constants of 450 K and 160 atmospheres are assumed. Thermodynamic data for 3:1 molar mixtures of hydrogen and nitrogen have been calculated by advanced corresponding states principle techniques using the two-fluid van der Waals model (Breedfeld and Prausnitz [6]). The calculations show that within the temperature and pressure ranges of interest in the present study, hydrogen-nitrogen mixtures deviate only to second order from ideal solution behaviour.

The general characteristics of the temperature-enthalpy curves for ammonia and for the complementary 3:1 hydrogen-nitrogen mixture associated with the reaction (3) are illustrated in Figure 2 below for a system pressure of 300 atmospheres. The complementary fluids are represented by the left and right extreme curves respectively, the gas mixture being characterised by essentially constant specific heat whereas the curves for ammonia exhibit pronounced curvature within the vaporization region. No definite boiling temperature is evident since the system pressure exceeds the critical pressure for ammonia.

Calculation of thermodynamic properties for intermediate mixtures of ammonia/hydrogen-nitrogen represents a formidable problem since ammonia is a polar fluid. Advanced corresponding states principle techniques that have been developed recently [6] can, however, cope with the problem within the high temperature single phase region, as shown elsewhere [5] by comparison between computed and observed heats of mixing. Ammonia/hydrogen-nitrogen mixtures behave essentially as regular solutions in the high temperature region above 800 K; that is, the mixing heat for a given mixture is finite but independent of temperature. This effect represents the macroscopic manifestation of the persistent intermolecular forces caused by the finite polarity of the ammonia molecules. Mixing heats at temperatures above 800 K increase from typically 1% to 3% of the reaction enthalpy for pressures in the range 100 to 300 atmospheres. In this study we adopt the approximation that within these ranges of temperature and pressure, mixing heats may be neglected; that is, mixtures within these ranges will always be treated as ideal solutions. It would be unwise to apply such an approximation to systems at higher pressure which deviate rather more strongly from ideality.

The only other thermodynamic data we have located within the literature suitable for the calculation of energy storage efficiencies for the ammonia/hydrogen-nitrogen system are phase equilibrium measurements by Michels et al [7] which define the compositions $x_l(T)$ and $x_g(T)$ of the liquid and gas phases within the two-phase region. The measurements are summarised in Figure 1, the left hand side of each curve representing the effect of the limited solubility of the gas mixture in ammonia and the

right hand side representing the effect of finite amounts of ammonia vapour within the gas phase. The equilibrium compositions $x_l$ and $x_g$ at T may be determined from the intersections of the phase equilibrium curve with the isotherm at T. We have been unable to locate data defining the system enthalpies $H(x_l)$ and $H(x_g)$ corresponding to the phase equilibrium compositions but show below that these may be generated by application of the separation work criterion developed in the following sections.

## 2.2 Separation Work Criterion

It was shown in [1] that separation work in a liquid/gas separating thermochemical energy transfer system is developed internally by degradation of mixing heat and indeed, for the general reaction (1), the work

$$W_s(x) = T_S \Delta S_m(x) \tag{5}$$

required for separation of a mixture at x into liquid and gas phases at $T_S$ comprising pure A and pure B respectively, is equal to the loop work defined by

$$W_L(x) = \int_{T_S}^{T_f} d[\Delta H^E(x,T)] \left(1 - \frac{T_S}{T}\right) \tag{6}$$

where $\Delta H^E(x,T)$ is the excess heat of mixing given by

$$\Delta H^E(x,T) = H(x,T) - (1 - \delta)H(0,T) - \delta H(1,T) \tag{7}$$

and where the temperature limit $T_f$ occurs within the ideal solution region at high temperatures; that is, within the region where the mixing heat given by (7) equals zero. The entropy of mixing in (5) is given by

$$\Delta S_m(x) = - \frac{Rm}{m(1 - x) + x} [x\ln x + (1 - x)\ln(1 - x)] \qquad (8)$$

The equality between equations (5) and (6) may be used as the basis of a criterion for determining values for mixture enthalpies H(x,T) throughout the temperature range of interest. Before this criterion may be developed, however, it is necessary to generalise equations (5), (6) and (7) to include the case where incomplete separation occurs at $T_S$; that is, to the case where finite amounts of gas are dissolved in the liquid phase at $T_S$, and vapour from the liquid component is present in the gas phase. The liquid and gas phases are characterised then not by the pure components A and B but by mixtures which we define respectively by mole fractions $x_{ls}$ and $x_{gs}$ of B. The temperature-enthalpy curves for the mixtures at $x_{ls}$ and $x_{gs}$ intersect the dew line defining the boundary between the single phase and two-phase regions at $T_S$, as shown in Figure 2.

In order to extend the analysis to the case of incomplete separation, we define a generalised excess heat of mixing at x referred to the extreme enthalpies at $x_{ls}$ and $x_{gs}$:

$$\overline{\Delta H^E}(x,T) = H(x,T) - (1 - \bar{\delta})H(x_{ls},T) - \bar{\delta}H(x_{gs},T) \qquad (9)$$

where

$$\bar{\delta} = \frac{\delta - \delta_{ls}}{\delta_{gs} - \delta_{ls}} \qquad (10)$$

Since no mixing occurs between phases, the mixing heat (9) is zero at $T_S$ and, by molar proportions, is zero also within the ideal solution region at high temperatures. It is therefore possible to identify a cyclic path, as illustrated in Figure 2, around which loop work at x may be calculated as

$$\overline{W_L}(x) = \int_{T_S}^{T_f} d[\overline{\Delta H^E}(x,T)] \left(1 - \frac{T_S}{T}\right) \tag{11}$$

The same arguments as presented in Section 4 of [1] may now be used to show that the loop work equals the separation work

$$\overline{W_S}(x) = T_S[\Delta S_m(x) - (1 - \bar{x})\Delta S_m(x_{ls}) - \bar{x}\Delta S_m(x_{gs})] \tag{12}$$

where $\Delta S_m(x)$ is given by (6) and where

$$\bar{x} = \frac{x - x_{ls}}{x_{gs} - x_{ls}} \tag{13}$$

The equality between the loop and separation work equations (11) and (12) may be used as a convenient criterion for testing the thermodynamic consistency of any trial curve defined by values of $H(x,T)$ as a representation of the temperature-enthalpy characteristic curve for the mixture at x. Given values of $H(x,T)$, the excess heat of mixing defined by (9) may be computed throughout the temperature range and hence a value determined for the loop work $\overline{W_L}(x)$ given by (11). The trial curve is thermodynamically consistent only when the loop work equals the separation work (12), a requirement which must extend over the

full spectrum of available mixtures between $x_{ls}$ and $x_{gs}$. Development of the iterative method for determining the consistent values of H(x,T) is described below in Section 2.4.

## 2.3 Generation of H(x,T) Values

In order to apply the above criterion it is necessary to generate trial values of H(x,T) and this may be accomplished in an ordered manner if a trial curve is initially defined for the dew line, as shown in Figure 2. Once the dew line is defined, then the phase equilibrium enthalpies $H_d(x_l)$ and $H_d(x_g)$ corresponding to the liquid and gas phases respectively are defined also at each temperature T within the two-phase region from the intersections between the dew line and the isotherm at T (given temperature-composition information, as shown for example in Figure 1). By assuming that no mixing occurs between phases, the enthalpy of any two-phase mixture at T may then be determined as

$$H(x,T) = (1 - \bar{\delta}_d)H_d(x_l) + \bar{\delta}_d H_d(x_g) \qquad (14)$$

where

$$\bar{\delta}_d = \frac{\delta - \delta_l}{\delta_g - \delta_l} \qquad (15)$$

The variables $\bar{\delta}_d$, $\delta_l$ and $\delta_g$ are all temperature dependent through the phase composition data for $x_l$ and $x_g$, as shown in Figure 1.

Values for H(x,T) are known from (14) within the two-phase region and also, from molar proportions, are known within the ideal solution region at high temperatures. Within the intermediate single phase region where mixing heats are finite, however, there is generally insufficient data in the literature to define mixture enthalpies. In order to complete the temperature-enthalpy curve defined by H(x,T) for a given mixture, it is therefore necessary to apply a suitable interpolation rule for connecting the ideal solution and two-phase regions.

Given that insufficient data is available for defining the exact shape of the temperature-enthalpy characteristics within the intermediate region and that further, no unusual variation is expected, we have adopted a simple quadratic interpolation rule based on values of H(x,T) at 800 K and 1000 K within the ideal solution region, and a third value defined by (14) at the single phase/two-phase boundary. The interpolation rule is illustrated in Figure 2. The rule has been applied to all mixtures except those at very low values of x corresponding to the left arms of the phase composition curves shown in Figure 1. As x tends towards zero, the values of H(x,T) must tend towards H(0,T) corresponding to pure ammonia and therefore the curvature of the characteristic curves becomes more pronounced within the vaporization region than can be adequately represented by a quadratic interpolation. Deviations from the quadratic interpolation rule were introduced in this region, based on the tendency towards the curvature of the pure ammonia characteristic curve. Rather greater uncertainty in the interpolation procedure is thereby also introduced, but only within a very small region at low x.

## 2.4 Application of the Separation Work Criterion

We have shown above that values of $H(x,T)$ may be generated provided that the dew line is defined. In this section we locate the thermodynamically consistent values of enthalpy corresponding to phase equilibrium, thus allowing the dew line to be positioned on the temperature-enthalpy diagram. In defining a trial curve for the dew line, we adopt the initial assumption that the mixtures comprising the liquid phase at low x obey Henry's law. Values of $H_d(x_1)$ and hence the left arm of the dew line shown in Figure 2 may thence be defined as

$$H_d(x_1) = (1 - \delta_1)H(0,T) + \delta_1 H(1,T) \qquad (16)$$

Since $x_1$ is small for the ammonia/hydrogen-nitrogen system, as shown in Figure 1, and since mixing heats are not expected to be large for solutions of gases in liquids, significant errors are not anticipated. Moreover, deviations from the assumption may be introduced by means of the iterative procedure described below.

The iteration adopted for positioning the dew line on the temperature enthalpy diagram is outlined in Figure 3. The left arm of the dew line is defined initially according to (16) and an arbitrary trial curve is then chosen to complete the phase boundary. At each x, values of $H(x,T)$ may then be generated according to the procedure described in Section 2.3, and the loop work $\overline{W}_L(x)$ hence computed from (9), (10) and (11). The reference temperature $T_S$ is initially chosen sufficiently low that the extreme mole fractions $x_1$ and $x_g$ in (9) approach zero and unity

respectively. For the ammonia/hydrogen - nitrogen system, $T_S$ is chosen equal to 250 K. If the loop work exceeds the separation work calculated from (12), then the dew line must be raised towards high temperatures in order to reduce the area of the loop shown in Figure 2. Conversely, if the separation work exceeds the loop work, the dew line must be moved towards lower temperatures. Thermodynamic consistency at each x is only obtained when the loop work equals the separation work.

The separation work criterion is applied first at high values of x, corresponding to low temperatures, and is then applied successively at lower values of x until the full span of the right arm of the dew line is defined. The left and right arms of the dew line must be connected smoothly so that a single continuous curve consistent with the phase composition data of Figure 1 is obtained. Fine adjustments to obtain a better correlation between loop and separation work are effected by varying the position of the left arm. The extent of correlation achieved for ammonia/hydrogen-nitrogen is shown in Figure 4. Here, the correlation corresponding to $T_S = 300°K$ is calculated directly from (11) and (12) on the basis of the dew line position evaluated from the earlier choice of $T_S = 250°K$. The 300 K correlation represents the better assessment of the procedure and shows that the requirement for thermodynamic consistency has been essentially satisfied. The small differences between separation and loop work seen in Figure 4 are only secondary and result from deviations from the assumed quadratic interpolation rule. Insufficient experimental data is available to justify development of a more accurate correlation at the present time.

## 2.5 Temperature-Enthalpy Characteristic Curves

A complete set of H(x,T) values covering all mixtures and all temperatures within the range of interest are generated by application of the separation work criterion, as shown in Figure 5. Corresponding thermodynamic information for Gibbs' free energies may be generated by use of the Gibbs'-Helmholtz relation

$$G(x,T) = \frac{T}{T_0}G(x,T_0) + T\int_{T_0}^{T} H(x,T)\,d\left(\frac{1}{T}\right) \qquad (17)$$

where $T_0$ is chosen sufficiently small that the liquid and gas phases are separated completely into ammonia and hydrogen-nitrogen respectively. In that case

$$G(x,T_0) = (1 - \delta)G(0,T_0) + \delta G(1,T_0) \qquad (18)$$

where $G(1,T_0)$ for the 3:1 hydrogen-nitrogen mixture includes the appropriate Gibbs' free energy of mixing. The equilibrium lines shown in Figure 5 are defined by the equilibrium mole fractions $x_e$ which may be evaluated for each T and P by applying the equilibrium condition

$$\left.\frac{\delta G(x,T)}{\partial \delta}\right|_{x_e} = 0 \qquad (19)$$

Complete tabulated thermodynamic data developed by the methods described in this paper are detailed elsewhere (Williams [8]).

The temperature-enthalpy characteristic curves comprise two distinct zones as seen in Figure 5. The dew line for each pressure has been positioned to within a fitting accuracy of

± 0.5 K, corresponding to a fitting accuracy of typically ± 50 cal/mole $NH_3$ for the H(x,T) values within the region near the phase boundary.

The only thermodynamic data we have located within the literature available for testing the validity of thermodynamic data generated by the present method has been recorded by Michels et al [9] for a single mixture of ammonia/ 3:1 hydrogen-nitrogen within the single phase region immediately above the dew line. This data is compared in Figure 6 to the predictions of the present analysis with good agreement being obtained, even to the extent that the correct variation of enthalpy with pressure is predicted. Lower values of specific heat are predicted by the present analysis but this discrepancy is not unexpected in view of the lack of information available for defining the interpolation rule required in the analysis. It is shown in the following section by comparison between experimental measurements of heat exchanger outlet temperatures and predictions from the present analysis that the assumed quadratic interpolation rule is quite adequate for the desired purpose of calculating energy storage efficiencies.

## 3. ENERGY STORAGE EFFICIENCIES

Energy storage efficiencies calculated from (2) for conditions of pure ammonia feed to the endothermic reactor and for $T_S$ chosen as 300°K are shown in Figure 7 as a function of endothermic reaction extent. The maximum value $\Delta H_{max}$ of enthalpy difference defining the denominator of (2) generally corresponds

to the dew temperature for the given mixture, as is evident from Figure 5. Energy storage efficiencies equal to unity are obtained for zero reaction extent and for values of $\delta$ greater than $\delta_g(T_S)$ since in each case no heat is available to waste to the environment. Energy storage efficiencies are less than unity for intermediate reaction extents and beyond the initial fall in value at low $\delta$ increase steadily towards unity as the reaction extent increases. A practical endothermic reactor would clearly need to be operated at high reaction extent, $\eta_{ST}$ being greater than 0.90 for ammonia/hydrogen nitrogen when $\delta$ exceeds 0.60 and increasing towards unity with increasing $\delta$. This result shows that energy storage efficiency is unlikely to represent a limiting factor in the development of thermochemical energy transfer systems for use in distributed solar power plants.

The energy storage efficiency calculations presented in this study may be tested by comparison with measurements originating from thermochemical energy transfer experiments performed in this laboratory. These experiments were designed to study the fundamental principles underlying the operation of a thermochemical solar absorber based on the ammonia dissociation reaction. The results are reported in detail elsewhere (Williams and Carden [10]). In the experiments, a stream of ammonia was passed through one side of a counterflow heat exchanger to an electrically heated reactor where it dissociated partially to form an ammonia/hydrogen-nitrogen mixture. The mixture was returned towards ambient temperatures by passage through the second channel of the heat exchanger. The exchanger was insulated against thermal losses and operated in standard manner with large

temperature differentials developed between the counterflow channels as a result of the differences between the specific heats of the two fluids. Heat is rejected from this system in the form of finite sensible heat carried by the fluid mixture passing from the outlet. The heat is wasted to the surroundings as the output fluid is piped from the heat exchanger. The corresponding value of energy storage efficiency is obtained as

$$\eta_{ST} = \frac{H(x,T_S) - H(0,T_S)}{H(x,T_o) - H(0,T_S)} \qquad (20)$$

where the numerator represents the chemical energy passed to storage and the denominator is the summation of the stored and lost energies. The heat exchanger inlet and outlet temperatures are defined by $T_S$ and $T_o$ respectively.

Given values of $\eta_{ST}$ such as in Figure 7 together with the thermodynamic data of Figure 5, it is possible to use equation (20) for predicting $T_o$ at chosen values of mixture composition, pressure and inlet temperature. The results of such predictions are shown in Figure 8 together with measured values of the heat exchanger outlet temperature. Temperature measurements are accurate to within $\pm 2^{\circ}C$ and composition measurements to within typically $\pm 2\%$. Although the extent of the data is somewhat limited (the experiment not being designed primarily for the present purpose), it is clear that the predictions reproduce the observed trends and lead us to the conclusion that the method adopted in this paper for generating thermodynamic data is satisfactory for the purpose of predicting energy storage efficiencies. In particular, we conclude that the calculation of

energy storage efficiencies is not limited by the lack of information for defining the exact form of the interpolation rule used in application of the separation work criterion. Further experiments covering a wider range of mixtures than that evident in Figure 8 and also based on more accurate temperature measurements would be required for a more rigorous comparison to test the sensitivity of the method to the form of the interpolation rule.

## 5. CONCLUSIONS

In this paper we have calculated energy storage efficiencies for a solar thermochemical energy transfer system by a method which requires generation of thermodynamic data not readily available in the literature. The method of generation is based on the use of phase equilibrium data for two-phase mixtures together with application of the thermodynamic criterion that the correct value of separation work for any given mixture should be generated internally within the system. We are not aware that this criterion has been applied previously. It is shown that energy storage efficiencies in excess of 90% may be obtained readily for a solar thermochemical energy transfer system based on ammonia dissociation/synthesis provided that the extent of the dissociation reaction exceeds 60%. It is not anticipated that any practical difficulties will be encountered in achieving this requirement.

## REFERENCES

[1] P O Carden and O M Williams, preceding paper, submitted to Int J of Energy Research.

[2] P O Carden, Solar Energy, 19, 365, (1977).

[3] American Institute of Physics Handbook (D E Gray, ed), 3rd edn, McGraw Hill, New York, (1972).

[4] Landholt-Bornstein tables, Band 4, Teil 4, Springer, Berlin, (1967).

[5] O M Williams, Energy Conversion Technical Report No 11, Department of Engineering Physics, The Australian National University, Canberra, ACT, Australia, (1976).

[6] G J F Breedfeld and J M Prausnitz, AIChEJ, 19, 783, (1973).

[7] A Michels, G F Skelton and E Dumoulin, Physica, 16, 831, (1950).

[8] O M Williams, Energy Conversion Technical Report No 16, Department of Engineering Physics, The Australian National University, Canberra, ACT, Australia, (1978).

[9] A Michels, T Wassenaar, G J Wolkers, W van Seventer and A J Venteville, Appl Sci Res, A4, 180, (1953).

[10] O M Williams and P O Carden, in preparation, to be submitted to Int J of Energy Research.

NOMENCLATURE

| | |
|---|---|
| A | Reactant species. |
| B | Product species. |
| $G(x,T)$ | System Gibbs' free energy at x, T and P, including reactant and product mixing terms. |
| $H(x,T)$ | System enthalpy at x, T and P. |
| $\Delta H(T)$ | Enthalpy difference between the heat exchanger feed and return fluids. |
| $\Delta H_{max}$ | Maximum value of $\Delta H(T)$ throughout temperature range. |
| $\Delta H^E(x,T)$ | Excess heat of mixing defined by (7). |
| $\overline{\Delta H^E}(x,T)$ | Excess heat of mixing defined by (9). |
| $H(x_l)$, $H(x_g)$ | Liquid and gas enthalpies defining the dew line. |
| m | Moles of B produced per mole of A consumed. |
| R | Gas constant. |
| P | System pressure. |
| $\Delta S_m(x)$ | Entropy of mixing at x. |
| T | Absolute temperature. |
| $T_S$ | Heat exchanger inlet temperature. |
| $T_o$ | Heat exchanger outlet temperature. |
| $T_f$ | Reference temperature wthin the ideal solution region. |
| $W_L(x)$, $\overline{W_L}(x)$ | Loop work defined by (6) and (11). |
| $W_S(x)$, $\overline{W_S}(x)$ | Separation work defined by (5) and (12). |
| x | Mole fraction. |
| $x_e$ | Equilibrium mole fraction. |
| $\bar{x}$ | Reduced mole fraction defined by (13). |

| | |
|---|---|
| $x_l(T)$, $x_g(T)$ | Liquid and gas mole fractions defining the dew line at T. |
| $x_{ls}$, $x_{gs}$ | Liquid and gas mole fractions defining the dew line at $T_S$. |
| $\delta$ | Weight fraction. |
| $\delta_l$, $\delta_g$ | Liquid and gas weight fractions defining the dew line at T. |
| $\delta_{ls}$, $\delta_{gs}$ | Liquid and gas weight fractions defining the dew line at $T_S$. |
| $\bar{\delta}$, $\bar{\delta}_d$ | Reduced weight fractions defined by (10) and (15). |
| $\eta_{ST}$ | Energy storage efficiency. |

FIGURE CAPTIONS

Figure 1 Phase composition measurements for ammonia/ 3:1 hydrogen-nitrogen from Michels et al [7].

Figure 2 Temperature-enthalpy characteristics for ammonia/3:1 hydrogen-nitrogen at 300 atmospheres illustrating the dew line position and the cyclic path from which the loop work at x is developed. The dashed line represents the molar proportions path of the virtual mixture and the dotted section of the true mixture path represents the quadratic interpolation referred to in the text.

Figure 3 Flow diagram outlining the iterative procedure for defining the position of the dew line at x on the temperature-enthalpy diagram.

Figure 4 Comparison between separation work calculated from the ideal solution formula (12) (full curves) and loop work calculated from (11).

o $T_S$ = 250 K

• $T_S$ = 300 K

Figure 5 Temperature-enthalpy characteristics for ammonia/ 3:1 hydrogen-nitrogen within the range 100-300 atmospheres.

Figure 6 Comparison between the predictions of the present analysis and the experimental measurements of Michels et al [9] for an ammonia/ 3:1 hydrogen-nitrogen mixture at $\delta = 0.64$.

- ● 100 atm.
- \+ 200 atm.
- o 300 atm.

Figure 7 Energy storage efficiencies for ammonia/ 3:1 hydrogen-nitrogen ($T_S$ = 300 K and pure ammonia feed.)

Figure 8 Comparison between observed and calculated heat exchanger outlet temperatures for ammonia/ 3:1 hydrogen-nitrogen.

- ● 100 atm
- \+ 150 atm
- o 200 atm

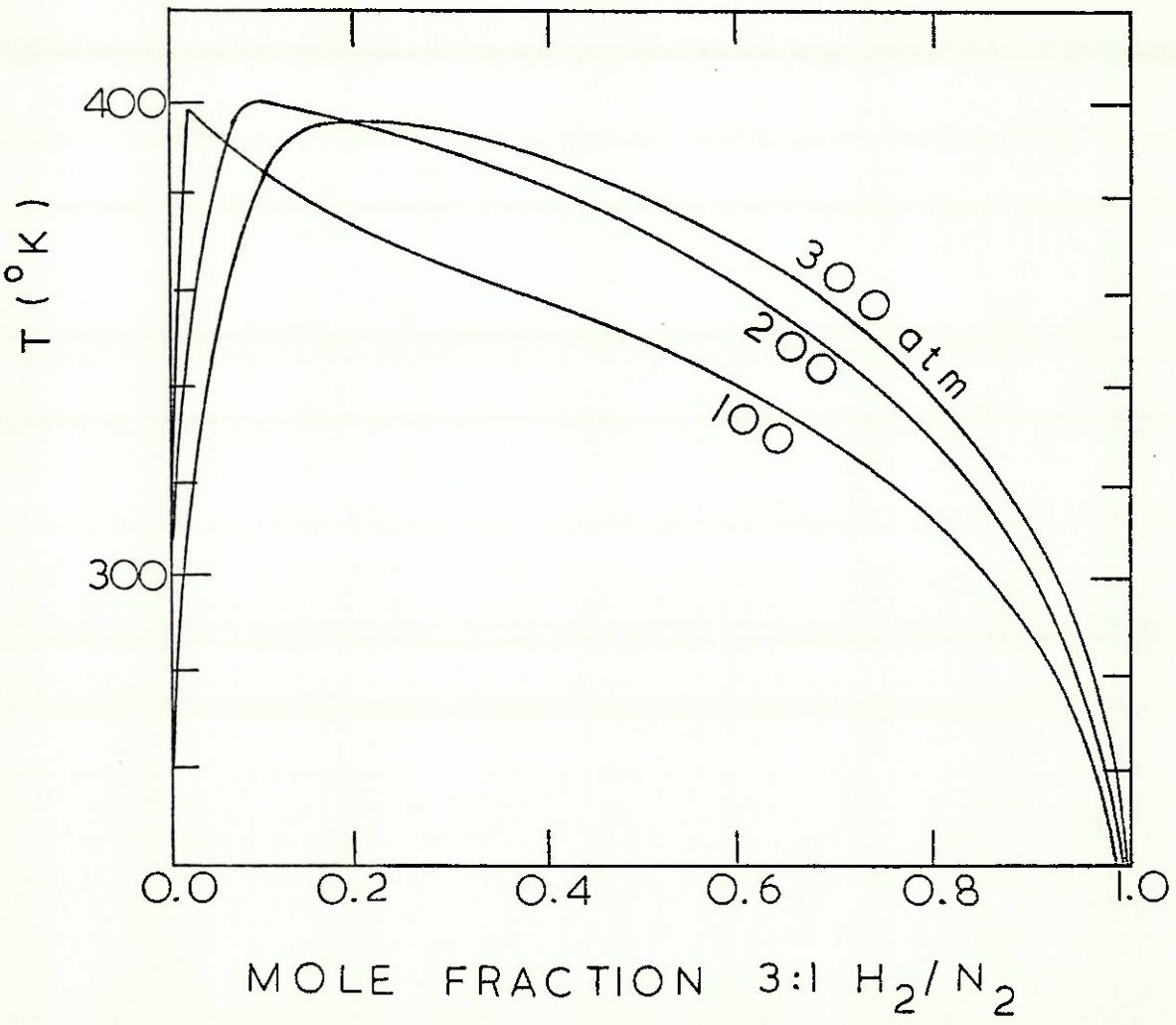


FIGURE 1: Phase composition measurements for ammonia/3:1 hydrogen-nitrogen from Michels et al [7].

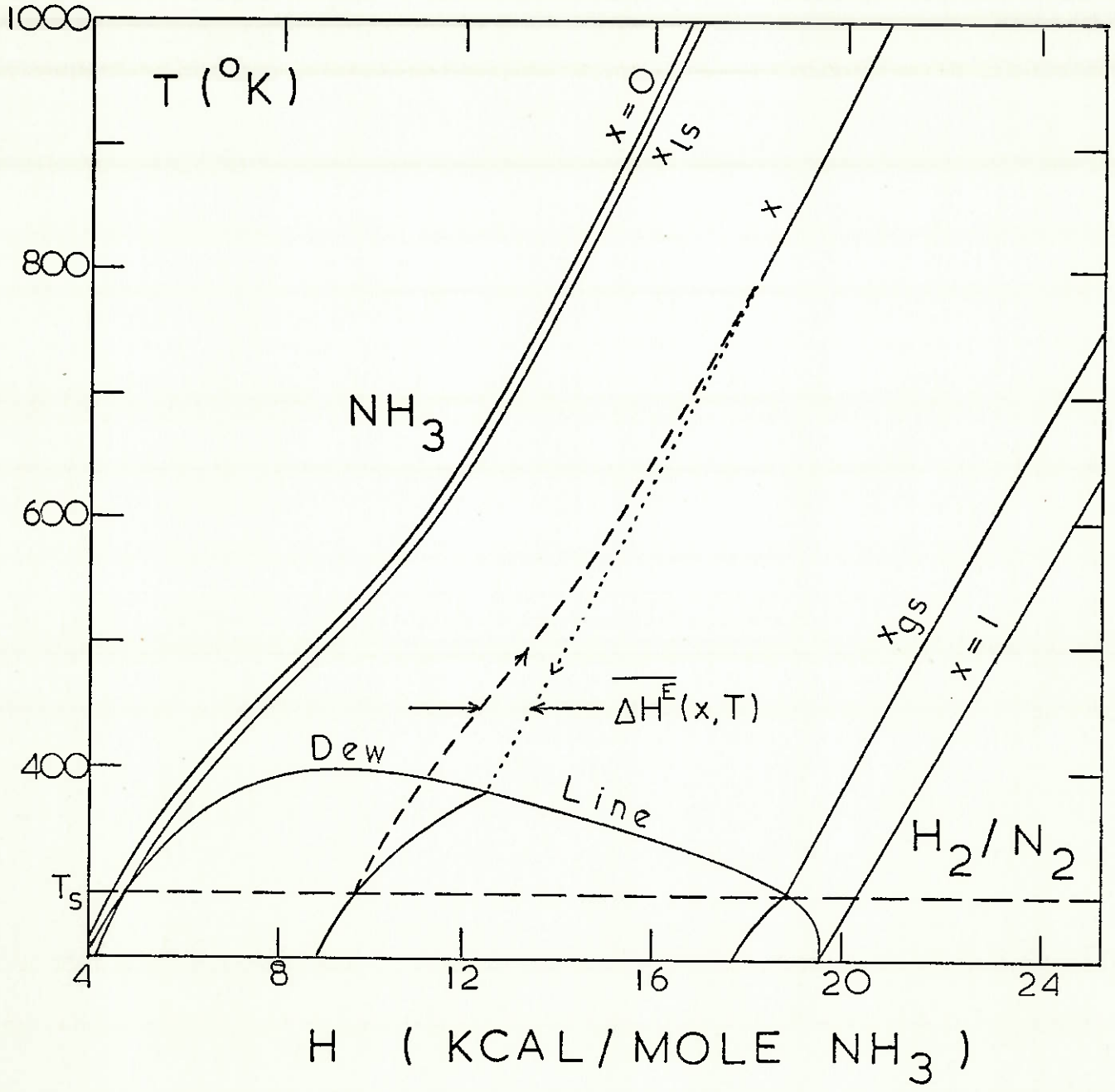


FIGURE 2: Temperature-enthalpy characteristics for ammonia/3:1 hydrogen-nitrogen at 300 atmospheres illustrating the dew line position and the cyclic path from which the loop work at x is developed. The dashed line represents the molar proportions path of the virtual mixture and the dotted section of the true mixture path represents the quadratic interpolation referred to in the text.

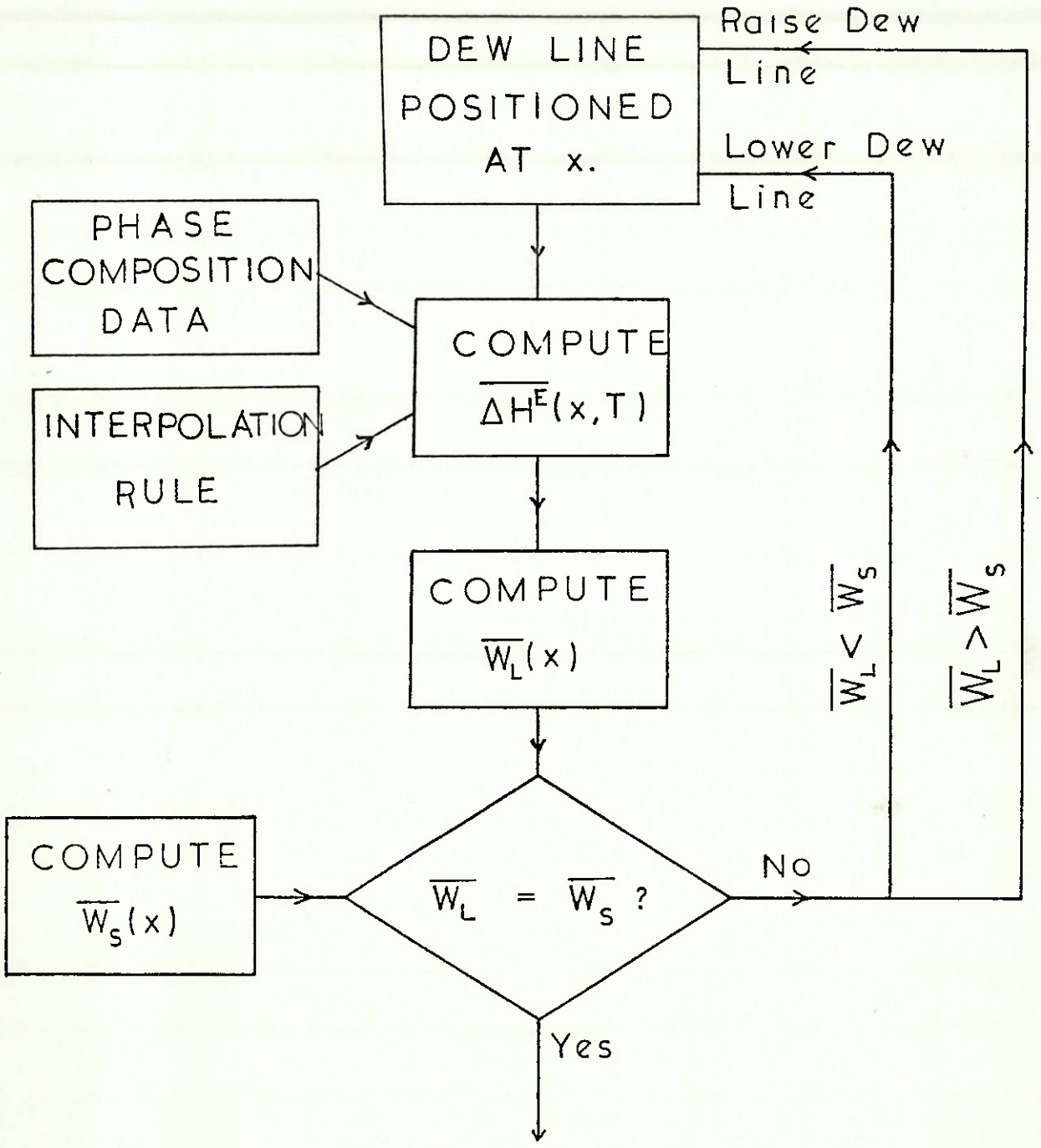


FIGURE 3: Flow diagram outlining the iterative procedure for defining the position of the dew line at x on the temperature-enthalpy diagram.

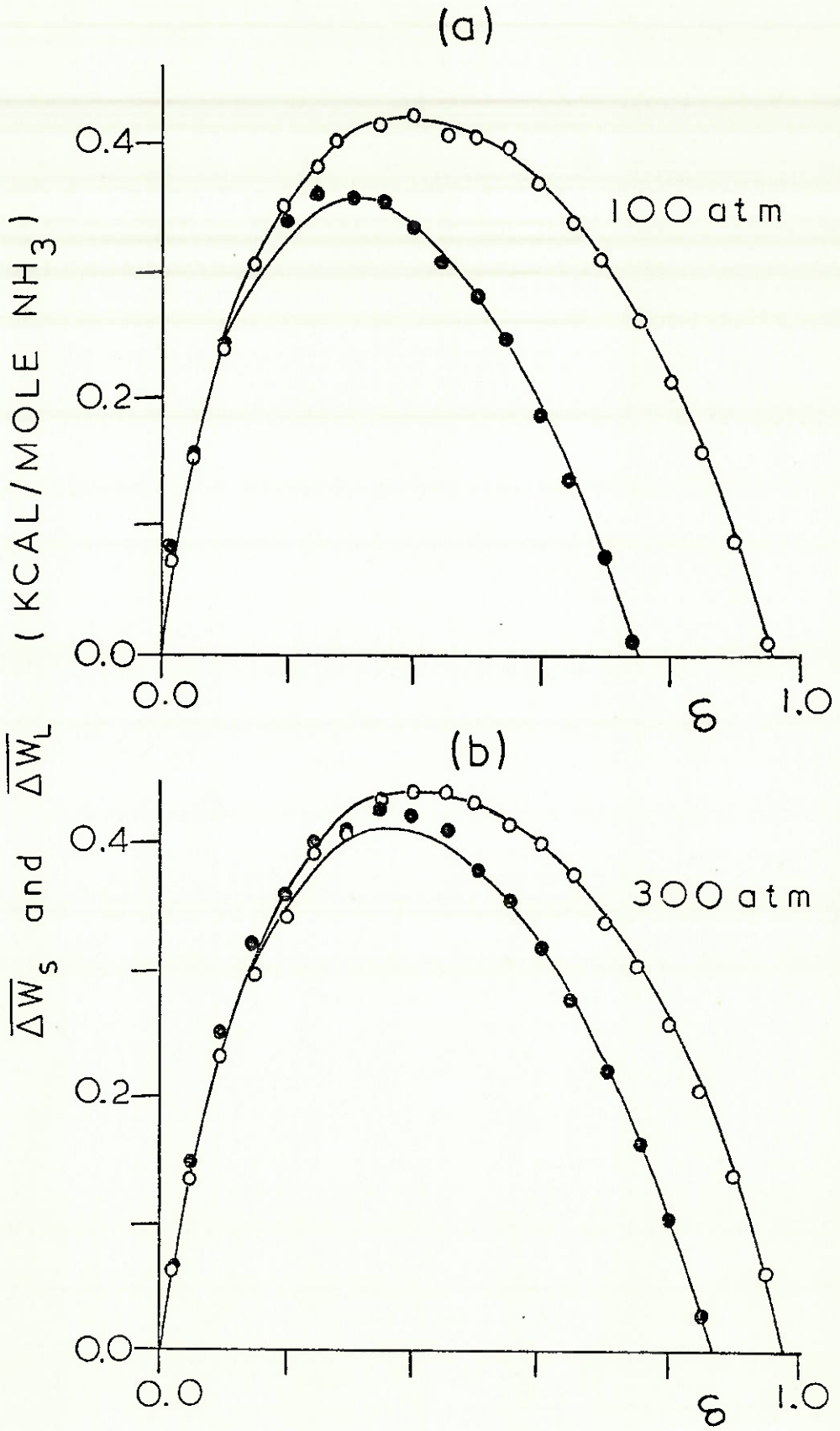


FIGURE 4: Comparison between separation work calculated from the ideal solution formula (12) (full curves) and loop work calculated from (11).

o $T_S = 250°K$

● $T_S = 300°K$

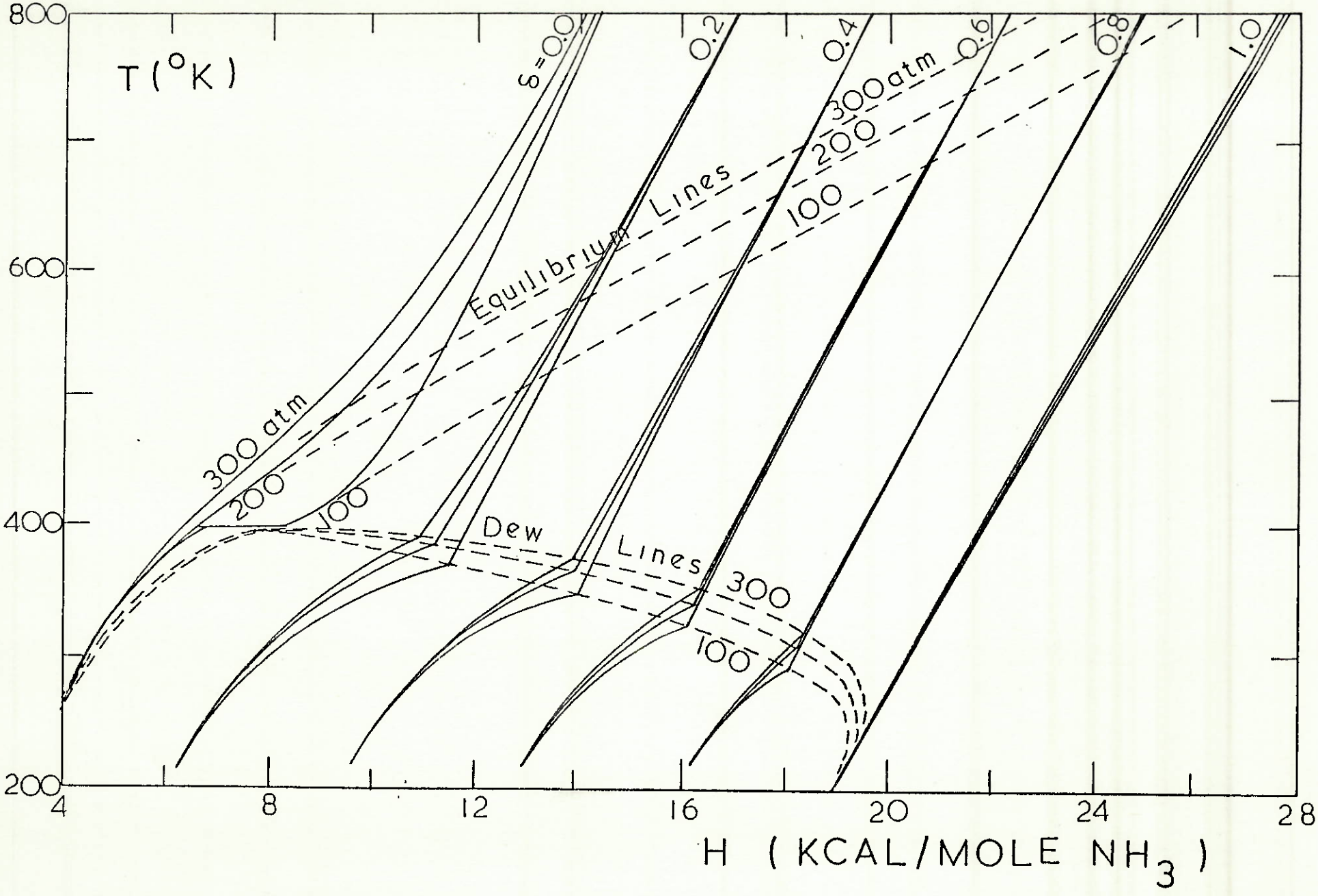


FIGURE 5: Temperature-enthalpy characteristics for ammonia/3:1 hydrogen-nitrogen within the range 100-300 atmospheres.

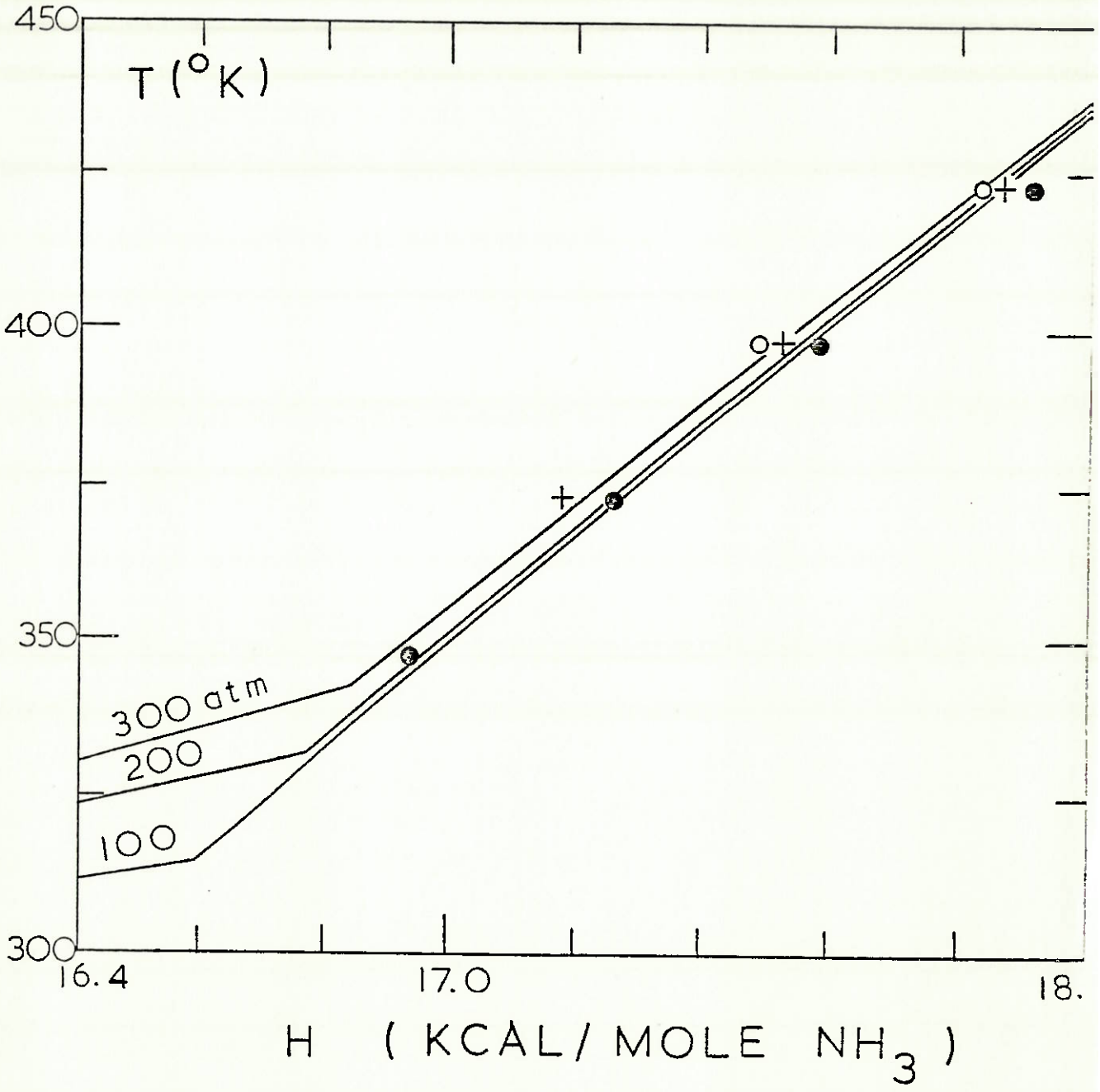


FIGURE 6: Comparision between the predictions of the present analysis and the experimental measurements of Michels et al [9] for an ammonia/3:1 hydrogen-nitrogen mixture at $\delta = 0.64$.

- ● 100 atm
- \+ 200 atm
- o 300 atm

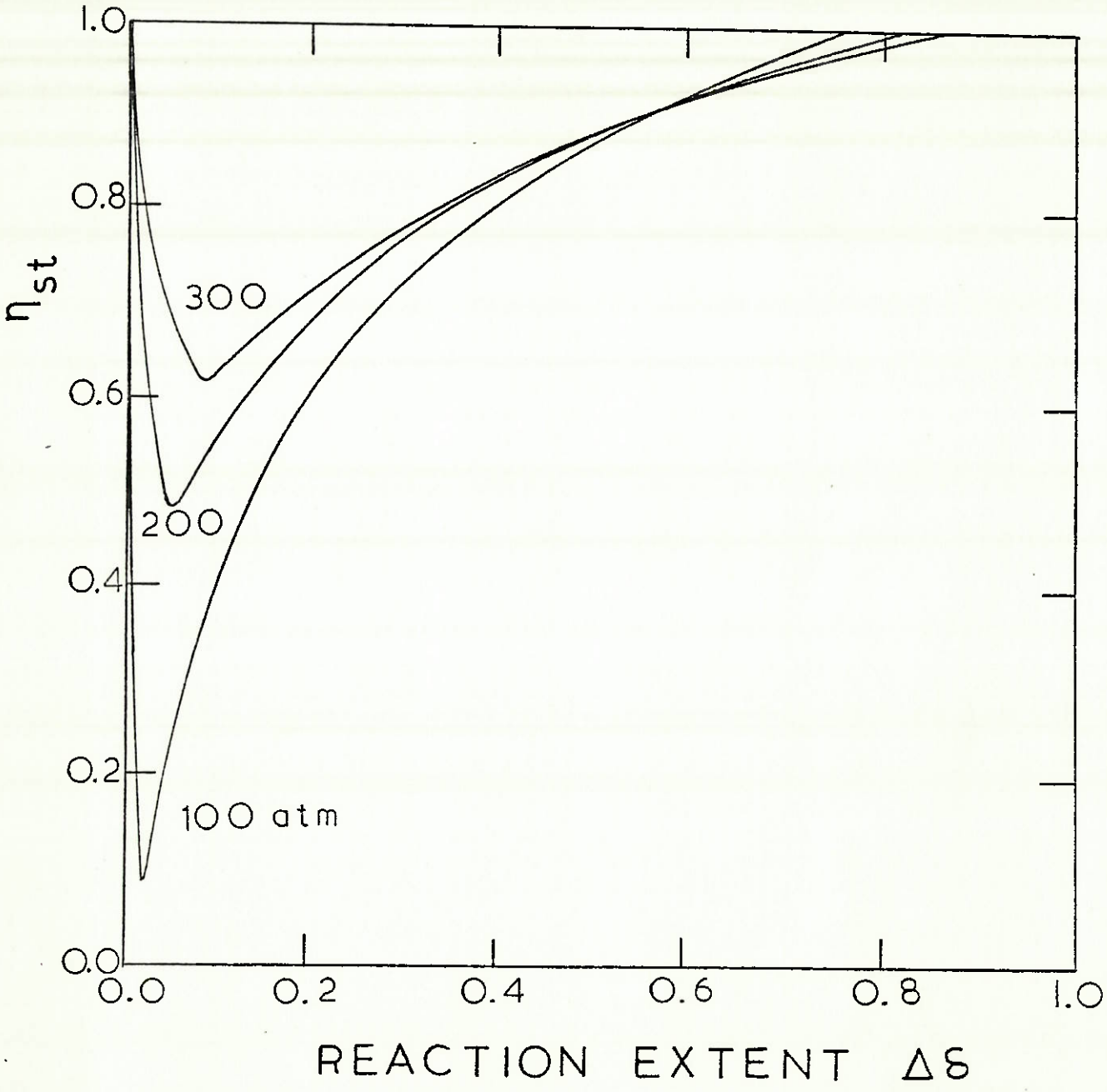


FIGURE 7: Energy storage efficiencies for ammonia/3:1 hydrogen-nitrogen ($T_S$ = 300°K and pure ammonia feed).

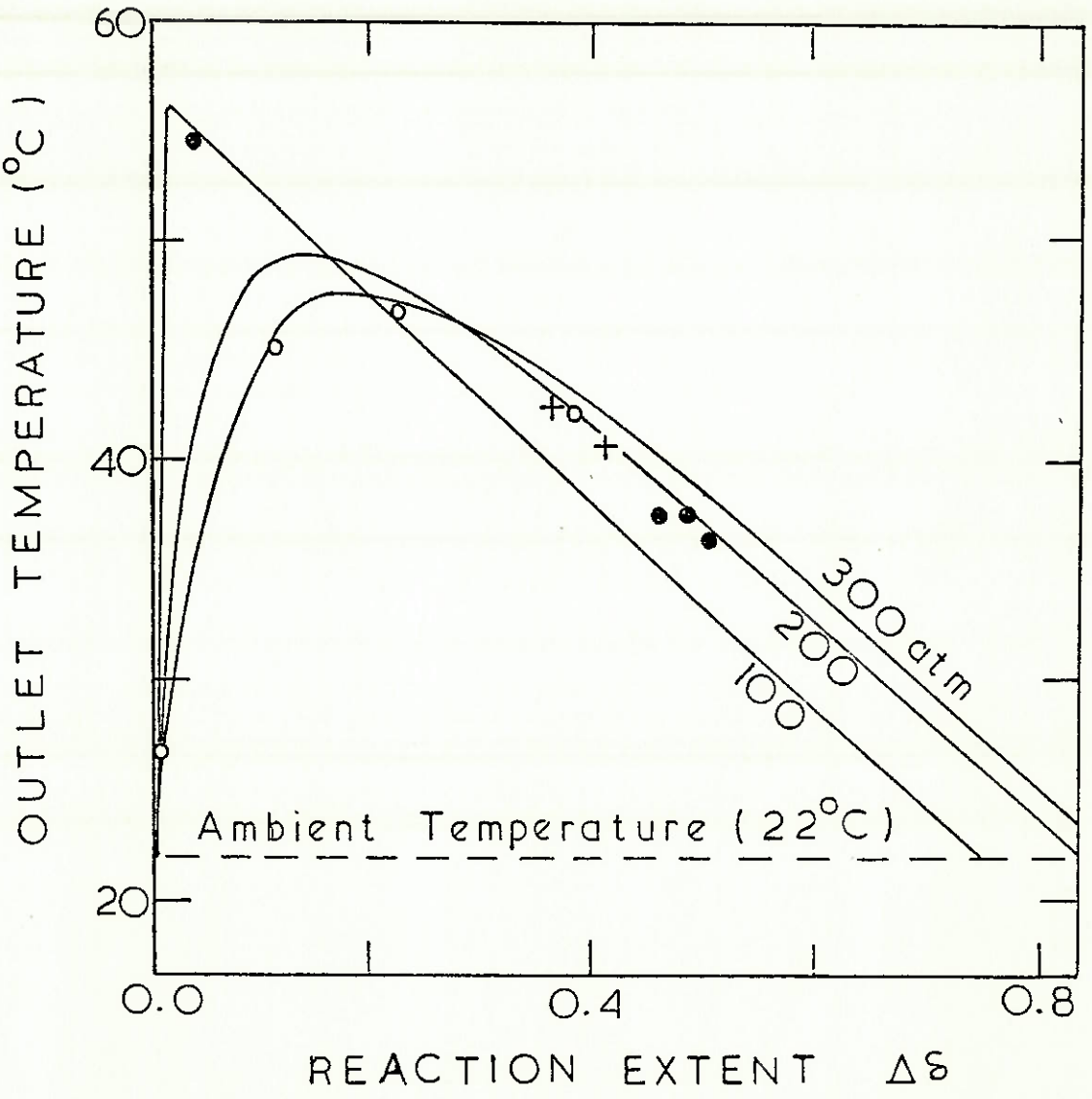


FIGURE 8: Comparison between observed and calculated heat exchanger outlet temperatures for ammonia/3:1 hydrogen-nitrogen

- ● 100 atm
- \+ 150 atm
- o 200 atm